Journal of Chromatography, 557 (1991) 469–479
Elsevier Science Publishers B.V., Amsterdam

CHROM. 23 098

Theoretical analysis for measurement of building pollution parameters by gas chromatography

N. A. KATSANOS* and Ch. VASSILAKOS
Physical Chemistry Laboratory, University of Patras, 26110 Patras (Greece)

ABSTRACT

The important parameters in gas–solid reactions can be determined simultaneously, under non-steady-state conditions using reversed-flow gas chromatography. A very simple experimental arrangement is required, with a slightly modified gas chromatograph. The distorted diffusion band obtained experimentally can be analysed mathematically giving, for the gas reactant, the values of adsorption, reaction and desorption rate constants, the overall mass transfer coefficients in the gas and in the solid and the adsorption equilibrium constant. All these parameters were determined at various temperatures for the reaction of sulphur dioxide with pieces of marble of two sizes, using two different air flow-rates.

INTRODUCTION

The main effects of air pollution on historic buildings and monuments are due to gas–solid reactions, and the important parameters in such reactions include the following:

(1) The rate constant for adsorption of the gas reactant on the external surface of the solid reactant, k_1.

(2) The overall mass transfer coefficient of the gas to the solid surface, K_G, related to k_1 by the equation

$$K_G = k_1 V'_G / A_s \tag{1}$$

where V'_G is the gaseous volume of void space in the solid bed and A_s is the total surface area of the solid.

(3) The rate constant for desorption of the gas reactant from the solid surface, k_{-1}.

(4) The overall mass transfer coefficient of the adsorbed gas in the solid, K_s, related to k_{-1} by

$$K_s = k_{-1} V_s / A_s \tag{2}$$

where V_s is the volume of the solid.

0021-9673/91/$03.50

(5) The adsorption equilibrium constant of the gas reactant between the solid and the gaseous phase:

$$K = K_G/K_s \tag{3}$$

(6) The first-order rate constant for the possible reaction of the adsorbed gas with the solid material, k_2.

If all above parameters can be measured simultaneously in the same experiment, under non-steady-state conditions, this will offer valuable information on the detailed mechanism of the action of air pollutants on historic buildings and monuments, thus providing a scientific basis for their conservation. This object can be achieved by employing reversed-flow gas chromatography (RF-GC), and it is the purpose of this paper to provide the necessary theoretical analysis so that the RF-GC technique be applied to the determination of the six parameters mentioned above.

The RF-GC method has been reviewed several times [1–4] and some more recent papers have been cited [5]. A preliminary synopsis of this paper has also been published [6].

THEORY

To help one follow the theoretical analysis, a brief description of the experimental outline is required, and is given in Fig. 1. Following the injection of a gaseous reactant, a diffusion current of it and of the possible gaseous products is set up inside column L_1, creating finite gas concentrations at the junction $x = l'$. On reversing the direction of the carrier gas flow at known times t_o, by means of the four-port valve, extra chromatographic peaks (sample peaks) appear superimposed on the continuous elution curve, thus forming a repeated sampling at $x = l'$ of

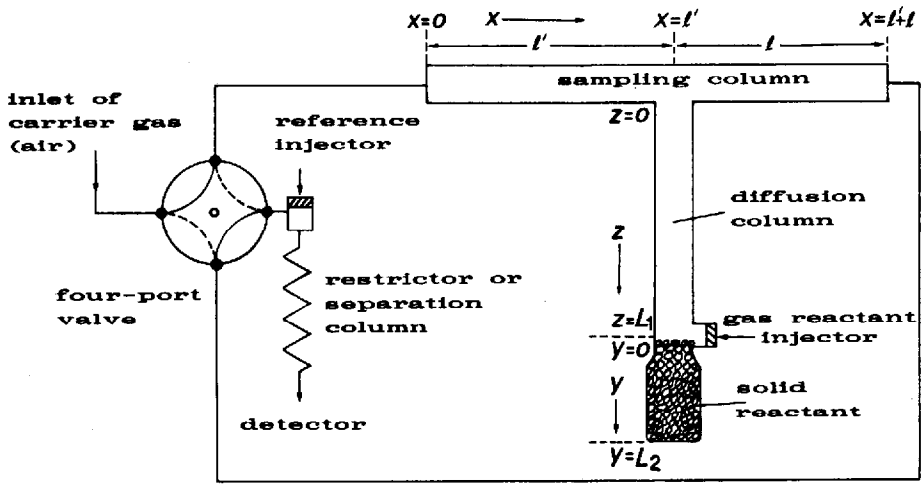

Fig. 1. Schematic representation of the columns and gas connections for studying gas–solid reactions by RF-GC under non-steady-state conditions.

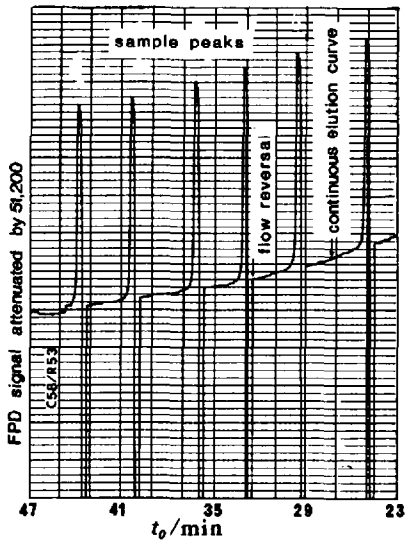

Fig. 2. Sample peaks due to simple flow reversals during the reaction of SO_2 with pieces of marble of 100–120 mesh at 323.2 K.

concentration $c(l', t_0)$ of the various substances present at this point at t_0. An example is given in Fig. 2.

The height h of the sample peaks, measured from the zero signal line, when plotted as $(1/m)\ln h$ *vs.* time t_0, where m is the response factor of the detector, gives a diffusion band, such as that shown in Fig. 3.

In the absence of any solid in vessel L_2 (*cf.*, Fig. 1), the diffusion band is determined by the geometric characteristics of the cell comprising sections l, l', L_1 and L_2, and the diffusion coefficient of the gas reactant into the carrier gas. When a solid

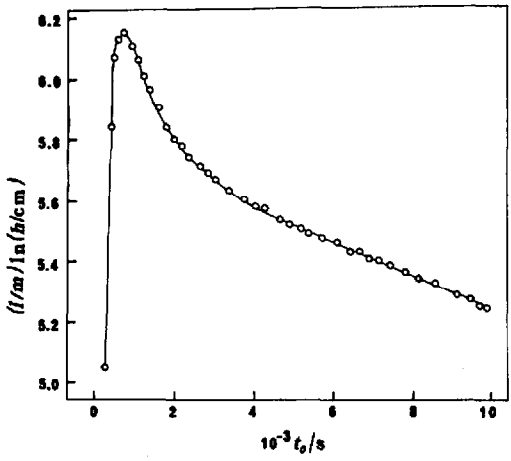

Fig. 3. A diffusion band for the reactant SO_2, obtained in the presence of pieces of marble (100–120 mesh) in vessel L_2 at 353.2 K.

reactant is present, the diffusion band is distorted in shape and/or in slope. It is this distortion which permits the calculation of the various kinetic and equilibrium parameters listed in the Introduction. The method is as follows.

The magnitude of $c(l', t_o)$ in each sampling act is related to the height h of the respective sample peak, measured from the baseline, by [4]

$$h = [2c(l', t_o)]^m \tag{4}$$

where m is the response factor of the detector. If $c(l', t_o)$ is found as an analytical function of the time, the mathematical equation describing the diffusion bands (previously mentioned) will be known. Under the slopes and the intercepts of these experimental bands are hidden all the physico-chemical parameters listed in the Introduction.

The function $c = c(l', t_o)$ has been derived in the past for many special cases pertaining to various physico-chemical parameters [4,5,7–11]. One particular publication [12] should be mentioned, as it deals with the same problem as that faced here, but under different experimental conditions and with different approximations. These led to the determination only of the adsorption rate constant k_1.

Now, one can combine, improve, modify and extend all the above derivations to serve the purposes of the present problem, adding the necessary new details to help readers follow the theoretical development.

The main idea of the technique, as outlined in Fig. 1, is to confine conventional chromatography used for separation purposes to the separation column, and reverse the direction of flow for sampling purposes only in the empty column $l' + l$. The effects of the gas–solid interaction in vessel y are not initially superimposed on the chromatographic stream running through the sampling and the separation column, but "sit" on the diffusion current of the reactant and the gaseous products into the carrier gas setting up inside the diffusion column z. The mathematical equation sought will be derived with the help of the coordinates in Fig. 1, by solving the diffusion equation first in the region z, then in the region y, and finally linking the two solutions by using appropriate boundary conditions at $z = L_1$ and $y = 0$.

Region z

The diffusion equation in this region is

$$\partial c_z/\partial t_o = D\partial^2 c_z/\partial z^2 \tag{5}$$

where $c_z = c_z(z, t_o)$ and D is the diffusion coefficient of the reactant into the carrier gas. If an amount m of the gas reactant is injected as an instantaneous pulse at $z = L_1$, the intial condition is

$$c_z(z, 0) = \frac{m}{a_G}\delta(z - L_1) \tag{6}$$

where a_G is the cross-sectional area in the columns z and $l' + l$ and δ is the Dirac delta function. The boundary conditions at $z = 0$ are

$$c_z(0, t_o) = c(l', t_o) \quad \text{and} \quad D(\partial c_z/\partial z)_{z=0} = vc(l', t_o) \tag{7}$$

where v is the linear velocity of the carrier gas in the sampling column. The solution of eqn. 5, with the initial condition 6 and subject to the boundary conditions 7, in the form of a Laplace transform with respect to time (parameter p_o), is

$$C_z = C(l', p_o)\cosh q_1 z + (v/Dq_1)C(l', p_o)\sinh q_1 z - (m/a_G Dq_1)\sinh q_1(z - L_1)\,u(z - L_1) \tag{8}$$

where

$$q_1^2 = p_o^0/D \tag{9}$$

and $u(z - L_1)$ is the unit step function. C_z and C denote the t_o Laplace-transformed functions of c_z and c, respectively.

For details of the derivation, see ref. 7.

Region y

The diffusion equation in this region is

$$\frac{\partial c_y}{\partial t_o} = D \cdot \frac{\partial^2 c_y}{\partial y^2} - \frac{K_s A_s}{V_G'}(c_s^* - c_s) \tag{10}$$

where c_y = concentration of the gaseous reactant in the gas phase of region y, c_s = concentration of the gaseous reactant adsorbed on the solid reactant, expressed in mol m^{-3}, c_s^* = concentration of the adsorbed reactant in equilibrium with that in the gas phase and D = diffusion coefficient of the gaseous reactant in the region y, assumed to be approximately equal to that in region z; for K_s, A_s and V_G' see Introduction.

The rate of change of c_s is given by

$$\frac{\partial c_s}{\partial t_o} = \frac{K_s A_s}{V_s}(c_s^* - c_s) - k_2 c_s \tag{11}$$

for V_s and k_2 see Introduction.

The system of eqns. 10 and 11, by applying Laplace transformation with respect to t_o, under the initial conditions $c_y(y, 0) = c_s(y, 0) = 0$, and then eliminating C_s between the transformed equations gives

$$d^2 C_y/dy^2 - q_2^2 C_y = 0 \tag{12}$$

where C_y is the transformed function c_y with respect to t_o, and q_2 is given by

$$q_2^2 = \frac{1}{D}\left(p_o + \frac{k_1 p_o + k_1 k_2}{p_o + k_{-1} + k_2}\right) \tag{13}$$

In proceeding from eqns. 10 and 11 to eqn. 12, eqns. 1, 2 and 3 were used, and also the definition $K = c_s^*/c_y$.

Eqn. 12 has been derived before [5,8], but not with the same content as here.

However, its solution is the same, *viz.*,

$$C_y'(0) = -C_y(0) q_2 \tanh q_2 L_2 \tag{14}$$

where $C_y(0)$ is the value of C_y at $y = 0$ and $C_y'(0) = (\mathrm{d}C_y/\mathrm{d}y)_{y=0}$.

Linking the solutions in regions z and y

Eqn. 8, valid in region z, is now linked with eqn. 14, holding in region y, by means of the boundary conditions at $z = L_1$ and $y = 0$, *viz.*, $C_z(L_1) = C_y(0)$ and $a_G(\partial C_z/\partial z)_{z=L_1} = a_G'(\partial C_y/\partial y)_{y=0}$, where a_G' is the cross-sectional area of the void fraction in region y. Using these two boundary conditions in eqn. 14, one obtains

$$(\partial C_z/\partial z)_{z=L_1} = -C_z(L_1)(a_G'/a_G) q_2 \tanh q_2 L_2$$

and calculating C_z and its z derivative at $z = L_1$ from eqn. 8, the result is

$$C(l', p_o) = \frac{m}{a_G D q_1}\left[\sinh q_1 L_1 + \frac{v}{Dq_1}\cdot\cosh q_1 L_1 + \frac{a_G'}{a_G}\cdot\frac{q_2}{q_1}\cdot\tanh q_2 L_2 \cdot \left(\cosh q_1 L_1 + \frac{v}{Dq_1}\cdot\sinh q_1 L_1\right)\right]^{-1} \tag{15}$$

This equation has exactly the same form as eqn. 21 in ref. 8, but the scientific content differs in that it now contains a gas–solid chemical reaction with rate constant k_2.

Approximations

In order that $c(l', t_o)$, and therefore h in eqn. 4, are found from eqn. 15, it is necessary to take the inverse Laplace transform of it. This can only be done, however, after introducing certain approximations in eqn. 15, most of which were used for an analogous equation recently [5], as follows:

(1) Omission of $\sinh q_1 L_1$ compared with $(v/Dq_1)\cosh q_1 L_1$, and also omission of $\cosh q_1 L_1$ compared with $(v/Dq_1)\sinh q_1 L_1$. Then eqn. 15 becomes

$$C(l', p_o) = \frac{m}{\dot{V}}\left[Dq_1 \sinh q_1 L_1 \left(\frac{\coth q_1 L_1}{Dq_1} + \frac{a_G' q_2}{a_G D q_1^2}\cdot\tanh q_2 L_2\right)\right]^{-1} \tag{16}$$

where $\dot{V} = v a_G$ is the volumetric flow-rate of the carrier gas.

(2) $Dq_1 \sinh q_1 L_1 \approx Dq_1 q_1 L_1 = L_1 p_o$

(3) $$\frac{\coth q_1 L_1}{Dq_1} \approx \frac{1}{L_1}\left(\frac{1}{p_o} + \frac{\pi^2}{3\beta}\right)$$

where

$$\beta = \pi^2 D/L_1^2 \tag{17}$$

(4) $\tanh q_2 L_2 \approx q_2 L_2$

Introducing approximations 2–4 into eqn. 16, it becomes, after rearrangement,

$$C(l', p_o) = \frac{m(\lambda + k'_{-1} + k'_2)}{\dot{V}\pi^2(^1/_3 + R)}\{\lambda^2 + [\pi^{-2}(^1/_3 + R)^{-1} + R(^1/_3 + R)^{-1}k'_1 + k'_{-1} + k'_2]\lambda + \pi^{-2}(^1/_3 + R)^{-1}(k'_{-1} + k'_2) + R(^1/_3 + R)^{-1}k'_1k'_2\}^{-1} \quad (18)$$

where

$$\lambda = p_o/\beta, \quad k'_1 = k_1/\beta, \quad k'_{-1} = k_{-1}/\beta, \quad k'_2 = k_2/\beta \quad (19)$$

β being the diffusion parameter, defined by eqn. 17, and

$$R = V'_G/V_G \quad (20)$$

i.e., the ratio of the gaseous volumes in vessel y (V'_G) and column z (V_G).

It should be noted that the time variable λ and the rate parameters k'_1, k'_{-1} and k'_2 are all dimensionless. The inverse transformation of eqn. 18 to find the analytical form of the function $c(l', t_o)$ depends on the relative values of the above four parameters. If the coefficient of λ in the denominator of eqn. 18 is set equal to

$$X = \pi^{-2}(^1/_3 + R)^{-1} + R(^1/_3 + R)^{-1}k'_1 + k'_{-1} + k'_2 \quad (21)$$

and the constant terms in the denominator are denoted by

$$(X^2 - Y^2)/4 = \pi^{-2}(^1/_3 + R)^{-1}(k'_{-1} + k'_2) + R(^1/_3 + R)^{-1}k'_1k'_2 \quad (22)$$

the two roots of the denominator are $-(X + Y)/2$ and $-(X - Y)/2$, and thus the inverse Laplace transformation of eqn. 18 gives the desired function of time as

$$c(l', t_o) = \frac{N_2}{2}\left[\left(1 + \frac{Z}{Y}\right)\exp\left(-\frac{X + Y}{2}\beta t_o\right) + \left(1 - \frac{Z}{Y}\right)\exp\left(-\frac{X - Y}{2}\beta t_o\right)\right] \quad (23)$$

where

$$N_2 = \frac{m\beta}{\dot{V}\pi^2(^1/_3 + R)} \quad (24)$$

and

$$Z = X - 2(k'_{-1} + k'_2) \quad (25)$$

This master equation, which has been derived in the same form for various other phenomena [3,5,7–10], the physical meaning of N_2, X, Y and Z being different each time, combines easily with eqn. 4 to give the mathematical description of distorted diffusion bands after the maximum, *i.e.*, only their descending branch (*cf.*, Experimental and Fig. 3).

Calculation of k_1, k_{-1}, k_2, K_G, K_s and K from the experimental data

The following steps are suggested for the calculation of these physico-chemical parameters, the meaning of which is explained in the Introduction.

(1) The value of the gaseous diffusion parameter β (eqn. 17) for each experimental arrangement and at each temperature is determined, by conducting an experiment without any solid in region y of the sampling cell (*cf.*, Fig. 1). The relevant diffusion band is constructed by plotting $(1/m)\ln h$ *vs.* t_o (*cf.*, Fig. 3), and the slope B_o of the last linear part after the maximum is computed. From this slope, β is found after division by r_2, $\beta = B_o/r_2$, where r_2 is the absolutely smaller root of the equation [9,10]

$$(1.29 + \pi^2 R)\lambda^2 + (4.29 + \pi^2 R)\lambda + 1 = 0 \tag{26}$$

and R is given by eqn. 20. Alternatively,

$$B_o = -\beta/\pi^2(^1/_3 + R) \tag{27}$$

as can be seen from eqn. 18 by setting $k'_1 = k'_{-1} = k'_2 = 0$ and taking the inverse transformation with respect to p_0. The result is

$$c(l', t_o) = N_2 \exp\left[-\frac{\beta}{\pi^2(^1/_3 + R)} t_o\right] \tag{28}$$

This coincides with eqn. 30 in ref. 5.

(2) An experiment is now conducted, under the same conditions as before, the only difference being that vessel y is filled with the solid reactant, as shown in Fig. 1.

The diffusion band is now distorted as compared with that of step 1, and is described (after the maximum) by eqn. 23. From the experimental band the two exponential coefficients $(X + Y)\beta/2$ and $(X - Y)\beta/2$, together with the two respective pre-exponential factors $N_2(1 + Z/Y)/2$ and $N_2(1 - Z/Y)/2$ are computed. This is done as described previously [5,7], *viz.*, by using a non-linear regression analysis computer program or, if the last part after the maximum is linear, by finding first the slope $-(X - Y)\beta/2$ and the intercept $\ln[N_2(1 - Z/Y)]$ of the last linear part of $(1/m)\ln h$ *vs.* t_o plot and then replotting the initial data of the non-linear part after the maximum as $(1/m)\ln\{h - N_2(1 - Z/Y)\exp[-(X - Y)\beta t_o/2]\}$ *vs.* t_o. Form the slope of the new straight line thus obtained, one finds $-(X + Y)\beta/2$ and from its intercept $\ln[N_2(1 + Z/Y)]$.

Dividing now the two slopes above by β, determined in step 1, one finds

$$B_1 = (X + Y)/2 \quad \text{and} \quad B_2 = (X - Y)/2 \tag{29}$$

By addition of these we find X and by subtraction we obtain Y:

$$B_1 + B_2 = X \quad \text{and} \quad B_1 - B_2 = Y \tag{30}$$

From the ratio ρ of the two pre-exponential factors, one finds

$$\rho = (1 - Z/Y)/(1 + Z/Y)$$

and from this

$$Z = \frac{1-\rho}{1+\rho} \cdot Y \tag{31}$$

The units used for the sample peak height, h, and any unknown proportionality factors do not influence the value of Z, as the latter is calculated from the ratio ρ of two intercepts pertaining to the same diffusion band.

(3) The values of X, Y and Z are now used in conjunction with eqns. 21, 22 and 25 to calculate the dimensionless rate constants k'_1, k'_2 and k'_{-1} with the help of the relationships

$$k'_1 = \frac{(X+Z)(^1/_3 + R) - 2\pi^{-2}}{2R} \tag{32}$$

$$k'_2 = \frac{(X^2 - Y^2)(^1/_3 + R) - 2(X-Z)\pi^{-2}}{2(X+Z)(^1/_3 + R) - 4\pi^{-2}} \tag{33}$$

$$k'_{-1} = X - \pi^{-2}(^1/_3 + R)^{-1} - R(^1/_3 + R)^{-1} k'_1 - k'_2 \tag{34}$$

The value of R used here is V'_G (packed)/V_G, in contrast to R in eqns. 26 and 27, which is V'_G (empty)/V_G.

The values of k_1, k_2 and k_{-1} are then found multiplying k'_1, k'_2 and k'_{-1} by β, respectively, according to the definitions 19.

(4) Finally, K_G, K_s and K are calculated from k_1 and k_{-1} by means of eqns. 1, 2 and 3, respectively.

EXPERIMENTAL

Materials and instruments

Sulphur dioxide and synthetic air, obtained form Linde Hellas (Athens, Greece), were of analytical-reagent grade. Marble was a sample from Penteli (Athens, Greece), approved as a reference material by the Commission of the European Communities.

A Pye Unicam (Cambridge, UK) PU 4500 gas chromatograph was used, equipped with a flame photometric detector. The sampling cell, consisting of the sampling column $l' + l$ (55 + 55 cm × 3.90 mm I.D.), the diffusion column L_1 (34.6 cm × 3.90 mm I.D.) and the vessel L_2 (5.1 cm × 18 mm I.D.), was accommodated inside the oven of the chromatograph. The carrier gas was dried with molecular sieve 12X.

Procedure

Before kinetic experiments, each marble sample was conditioned *in situ* by heating it at 200°C for 48 h, under a continuous carrier gas flow at a flow-rate of 0.283 or 0.583 cm^3 s^{-1}. Subsequently, the oven was adjusted to the working temperature and kept there overnight. Column L_1 was then filled with a uniform sulphur dioxide concentration by injecting into it 20 cm^3 of pure sulphur dioxide at atmospheric pressure. This was left for 1–2 days, until the signal at the detector decayed to a negligible height. Finally, 1 cm^3 of a gas mixture consisting of sulphur dioxide and

carrier gas (24%, v/v) was introduced through the injector, under a carrier gas flow, and the kinetic experiment was conducted by repeatedly reversing the flow direction at known times from the moment of injection.

The detector temperature was always 175°C and the pressure inside the cell was 1.04–1.05 atm (0.1054–0.1064 MPa).

RESULTS AND DISCUSSION

The methodology and equations given under Theory were applied to the action of sulphur dioxide at low concentrations in the carrier gas (synthetic air) on particles of Greek marble.

An example of the diffusion band for this particular case has already been given in Fig. 3. The response factor of sulphur dioxide for the flame photometric detector used had been determined previously [12], and its mean value was 1.92.

The values of the six physico-chemical parameters, calculated as described under Theory, are listed in Tables I and II for two sizes of marble particles, two flow-rates of the carrier gas, and four or five temperatures. It can be seen that there is a tendency for k_1 to decrease at the same temperature with increasing flow-rate of the air carrier gas, and this decrease is greater with marble particles of size 100–120 mesh, which have a larger specific surface area. Also, most of the other parameters for this size of particles decrease with increase in flow-rate, particularly at low temperatures. The changes observed when particles of size 22–30 mesh are used are less pronounced.

The negative values for k_2 observed with the smaller particles and a high flow-rate could mean that a chemical process leading to the release of sulphur dioxide from the marble is taking place, like the reverse of a chemisorption step.

In order that definite conclusions can be drawn about the mechanism of this particular gas–solid reaction, more experiments are required with other particle sizes

TABLE I

RATE CONSTANTS FOR ADSORPTION (k_1), DESORPTION (k_{-1}) AND CHEMICAL REACTION (k_2), MASS TRANSFER COEFFICIENTS IN THE GAS (K_G) AND IN THE SOLID (K_s), AND ADSORPTION EQUILIBRIUM CONSTANT (K) FOR THE GAS–SOLID REACTION OF SO_2 WITH MARBLE PARTICLES OF 22–30 MESH

T(K)	$10^5 k_1$ (s^{-1})	$10^5 k_{-1}$ (s^{-1})	$10^5 k_2$ (s^{-1})	$10^{10} K_G$ ($m\,s^{-1}$)	$10^{10} K_s$ ($m\,s^{-1}$)	K
Dry air as carrier gas with $V = 0.283$ $cm^3\,s^{-1}$						
323.2	11.2	5.70	7.32	2.99	1.82	1.65
353.2	13.2	8.52	6.00	3.51	2.72	1.29
373.2	14.2	5.93	7.39	3.77	1.89	1.99
393.2	13.2	7.52	7.36	3.51	2.40	1.46
423.2	17.1	8.46	10.46	4.55	2.70	1.69
Dry air as carrier gas with $V = 0.583$ $cm^3\,s^{-1}$						
323.2	9.77	4.88	7.75	2.59	1.55	1.66
353.2	10.56	7.05	5.43	2.81	2.24	1.25
373.2	8.33	6.58	3.65	2.21	1.16	1.90
393.2	12.92	8.77	6.09	3.43	2.79	1.23
423.2	16.30	7.94	10.46	4.33	2.53	1.71

TABLE II

RATE CONSTANTS FOR ADSORPTION (k_1), DESORPTION (k_{-1}) AND CHEMICAL REACTION (k_2), MASS TRANSFER COEFFICIENTS IN THE GAS (K_G) AND IN THE SOLID (K_s), AND ADSORPTION EQUILIBRIUM CONSTANT (K) FOR THE GAS–SOLID REACTION OF SO_2 WITH MARBLE PARTICLES OF 100–120 MESH

T(K)	$10^5 k_1$ (s^{-1})	$10^5 k_{-1}$ (s^{-1})	$10^5 k_2$ (s^{-1})	$10^{10} K_G$ ($m\,s^{-1}$)	$10^{10} K_s$ ($m\,s^{-1}$)	K
Dry air as carrier gas with $V = 0.283$ $cm^3\,s^{-1}$						
323.2	10.5	8.00	3.09	1.94	1.78	1.10
353.2	17.8	8.89	5.23	3.30	1.97	1.67
373.2	19.1	8.32	6.80	3.54	1.85	1.92
393.2	19.9	9.31	8.20	3.68	2.07	1.79
423.2	21.0	10.98	8.41	3.89	2.44	1.60
Dry air as carrier gas with $V = 0.583$ $cm^3\,s^{-1}$						
323.2	7.26	2.44	9.48	1.34	0.54	2.48
353.2	5.14	9.79	−1.04	0.95	2.17	0.43
393.2	7.58	12.82	−2.19	1.40	2.84	0.49
423.2	5.90	13.99	−2.23	1.09	3.10	0.35

or with single pieces of marble having particular shape, such as a sphere, cube, cone, cylinder or prism. Also, experiments with carrier gases loaded with water vapour should be conducted. Such work is in progress to elucidate the mechanism of the action of sulphur dioxide on marble.

ACKNOWLEDGEMENTS

This work was supported by a contract (No. EV 4V-0049 GR) of Environment and Waste Recycling of the Directorate-General for Science, Research and Development of the Commission of the European Communities, for which the authors express their gratitude. They also acknowledge the assistance provided by Mrs. M. Barkoula.

REFERENCES

1 N. A. Katsanos and G. Karaiskakis, *Adv. Chromatogr.*, 24 (1984) 125.
2 N. A. Katsanos and G. Karaiskakis, *Analyst (London)*, 112 (1987) 809.
3 N. A. Katsanos, *J. Chromatogr.*, 446 (1988) 39.
4 N. A. Katsanos, *Flow Perturbation Gas Chromatography*, Marcel Dekker, New York, Basle, 1988.
5 N. A. Katsanos and J. Kapolos, *Anal. Chem.*, 61 (1989) 2231.
6 N. A. Katsanos, G. Karaiskakis and Ch. Vassilakos, *Pure Appl. Chem.*, 61 (1989) 2057.
7 N. A. Katsanos and E. Dallas, *J. Phys. Chem.*, 91 (1987) 3103.
8 N. A. Katsanos, P. Agathonos and A. Niotis, *J. Phys. Chem.*, 92 (1988) 1645.
9 J. Kapolos, N. A. Katsanos and A. Niotis, *Chromatographia*, 27 (1989) 333.
10 N. A. Katsanos and J. Kapolos, in M. L. Occelli and R. G. Anthony (Editors), *Hydrotreating Catalysts*, Elsevier, Amsterdam, 1989, p. 211.
11 N. A. Katsanos and Ch. Vassilakos, *J. Chromatogr.*, 471 (1989) 123.
12 N. A. Katsanos and G. Karaiskakis, *J. Chromatogr.*, 395 (1987) 423.